ACS Catalysis

Research Article

pubs.acs.org/acscatalysis

Mechanism for the Carboxylative Coupling Reaction of a Terminal Alkyne, CO_2, and an Allylic Chloride Catalyzed by the Cu(I) Complex: A DFT Study

Ruming Yuan[†,‡] and Zhenyang Lin*[,†]

[†]Department of Chemistry, The Hong Kong University of Science and Technology, Clear Water Bay, Kowloon, Hong Kong, People's Republic of China

[‡]Department of Chemistry, Xiamen University, Xiamen 361005, People's Republic of China

Supporting Information

ABSTRACT: DFT calculations have been carried out to study the detailed mechanisms for carboxylative-coupling reactions among terminal alkynes, allylic chlorides, and CO_2 catalyzed by N-heterocyclic carbene copper(I) complex (IPr)CuCl. The competing cross-coupling reactions between terminal alkynes and allylic chlorides have also been investigated. The calculation results show that a base-assisted metathesis of (IPr)CuCl with PhC≡CH occurs as the first step to give the acetylide (IPr)Cu−C≡CPh, from which CO_2 insertion and reaction with an allylic chloride molecule, respectively, lead to carboxylative-coupling and cross-coupling reactions. It was found that both the reactions of (IPr)Cu−C≡CPh and (IPr)CuOCOC≡CPh (a species derived from CO_2 insertion) with an allylic chloride molecule occur through an S_N2 substitution pathway. The two S_N2 transition states (calculated for the carboxylative coupling and cross coupling) are the rate-determining transition states and show comparable stability. How the reaction conditions affect the preference of one pathway over the other (carboxylative coupling versus cross coupling) has been discussed in detail.

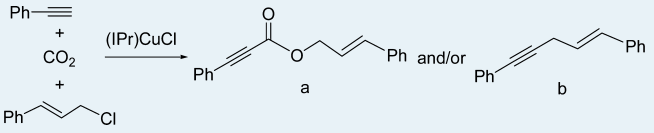

KEYWORDS: *carbon dioxide, terminal alkynes, copper(I) catalyst, carboxylative coupling, cross coupling, DFT study*

INTRODUCTION

The greenhouse effect has been recognized as an important environmental issue, and CO_2 makes up a significant percent of total greenhouse gas (GHG) emissions.[1,2] However, CO_2 is an attractive building block for organic synthesis because of its low cost and abundance.[3−5] Recently, significant efforts have been devoted to converting CO_2 into carboxylic acids and derivatives.[6,7] Compared to much-studied carboxylation reactions used to prepare carboxylic acids,[7,8] carboxylative coupling for directly producing carboxylic esters has been rarely reported.[9,10]

In 2010, Lu et al. reported that three-component carboxylative coupling among terminal alkynes, allylic chlorides, and CO_2 can be catalyzed by N-heterocyclic carbene copper(I) complex (IPr)CuCl to form carboxylative esters.[10] Equation 1 gives a representative example of the reactions. The experimental study by Lu et al. showed that in addition to major product a (carboxylative coupling product), in most cases, cross-coupling byproduct b is also produced (eq 1). In the experimental study, it has been found that relatively high CO_2 pressure (1.5 MPa) is beneficial to suppressing the formation of cross-coupling byproducts and significantly improving the rate of the carboxylative-coupling reactions. These findings are interesting and lead us to study the mechanism of the reactions.

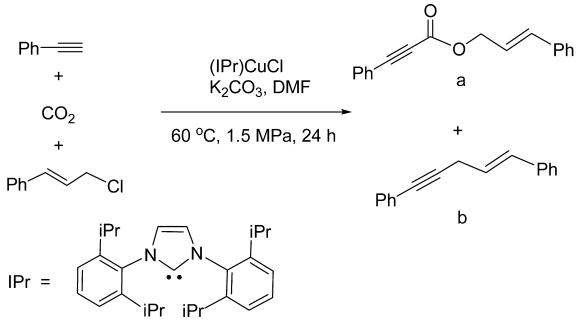

(1)

Scheme 1 shows the currently proposed reaction mechanisms for the two possible reaction pathways leading to carboxylative-coupling and cross-coupling reactions.[10−12] LCuCl first reacts with a terminal alkyne in the presence of a base to give copper(I) acetylide intermediate LCuC≡CPh. In the carboxylative-coupling cycle, CO_2 inserts into the metal−carbon bond of the acetylide intermediate to form a carboxylate intermediate, which then reacts with the allylic chloride to produce the carboxylative-coupling product (ester PhC≡CCOOCH$_2$CH=CHPh). In the cross-coupling cycle, a direct coupling between the copper(I) acetylide intermediate and the allylic chloride occurs to give the cross-coupling product

Received: August 1, 2014
Revised: October 11, 2014
Published: October 31, 2014

   dx.doi.org/10.1021/cs5011184 | ACS Catal. 2014, 4, 4466−4473

Scheme 1. Proposed Mechanisms for Carboxylative Coupling and Cross Coupling

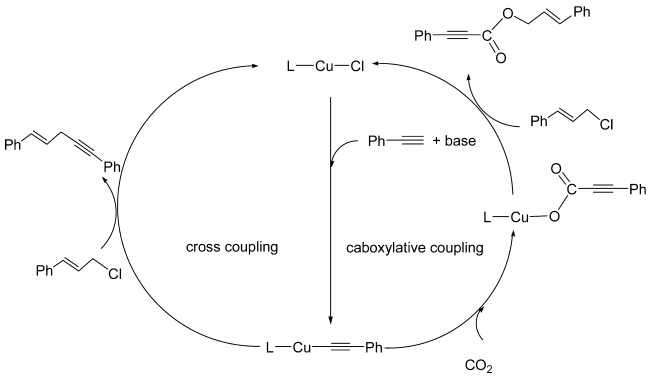

(PhC≡CCH$_2$CH═CHPh). However, details regarding the mechanisms are still not clear.

In this article, with the aid of DFT calculations, we examine in detail the mechanisms of the carboxylative-coupling and cross-coupling reactions shown in eq 1. Through these studies, we hope to answer the following questions: (1) What is the role of the base? (2) How does the main reaction pathway, which is carboxylative-coupling, compete against the cross-coupling pathway? (3) How do the couplings occur, via an S_N2 mode or an oxidative addition/reductive elimination mode? (4) How does high pressure help to improve the rate of carboxylative coupling, and how does temperature influence the reactions? These questions are very important for us to understand the reactions better.

COMPUTATIONAL DETAILS

The reactions studied in this article involve the formation of C−C and C−O bonds and the cleavage of C−Cl bonds. In an early study, Li et al. found that compared to other DFT methods, the B3P86 method gives good results on the dissociation enthalpies of these bonds.[13] Thus, B3P86, which employs the Becke88 exchange functional in combination with the gradient corrections of Perdew plus his 1981 local correlation functional, was used in all of our calculations.[14] The 6-311+G (d) basis set was used for Cu, Cl, and O atoms, and the 6-31G (d,p) basis set was used for all other atoms (C, H, N, and K).[15,16] In addition, the polarizable continuum model (PCM) was chosen to account for the solvent effect.[17] Corresponding to the experimental conditions, *N*,*N*-dimethylformamide (DMF) was adopted as the solvent. Because the steric effect is very important, we use full ligand IPr in all of the calculations. All of the structures were fully optimized in DMF solution and visualized using the XYZViewer software developed by de Marothy.[18] Vibrational frequencies were calculated analytically to ensure that a local minimum (LM) has no imaginary frequency (IF) and every transition state (TS) has only a single IF. Intrinsic reaction coordinates (IRC)[19] were calculated for the transition states to confirm that such structures indeed connect two relevant minima. To reduce the overestimation of the entropy contribution of the results, we also employed a correction of −2.6 (or 2.6) kcal/mol for 2:1 (or 1:2) transformations as many earlier theoretical studies did.[20] Unless specified, energies reported here are entropy-corrected free energies at 298 K. All quantum calculations were carried out with the Gaussian 09 program.[21]

We also employed the dispersion-corrected DFT method (B3P86-D2) to optimize all of the intermediates and transition states. For comparison, the relative energies calculated from B3P86 and B3P86-D2 are given in Table S1 in the Supporting Information. All of the structures calculated from the two methods are plotted side by side and are given in Figure S1. Energy profiles for the two most favorable pathways obtained from the two methods are compared and given in Figures S2. Single-point energy calculations using a larger basis set (6-311++G(d,p)) were also performed. The relative energies using the larger basis set are also given in Table S1. The results show that the large basis set in general gives slightly higher reaction barriers by up to 4 kcal/mol than does the medium basis set. However, the differences in the barriers among different reaction pathways do not change significantly.

Structurally, the two methods give similar results. The structures calculated from the two methods do not differ significantly (Figure S1). When we come to consider the energetic aspect, we make the following observations. (i) The most favorable pathways for carboxylative coupling and cross coupling predicted by B3P86 are the same as those predicted by B3P86-D2. (ii) The B3P86 results indicate that carboxylative coupling and cross coupling are competitive, in good agreement with the experimental observation. (iii) The B3P86-D2 results indicate that cross coupling is more favorable than carboxylative coupling, which is inconsistent with the experimental observation. (iv) The overall reaction barrier calculated for carboxylative coupling is 25.1 kcal/mol (B3P86) versus 18.3 kcal/mol (B3P86-D2), and the

Scheme 2. Detailed Catalytic Cycles for Carboxylative Coupling and Cross Coupling

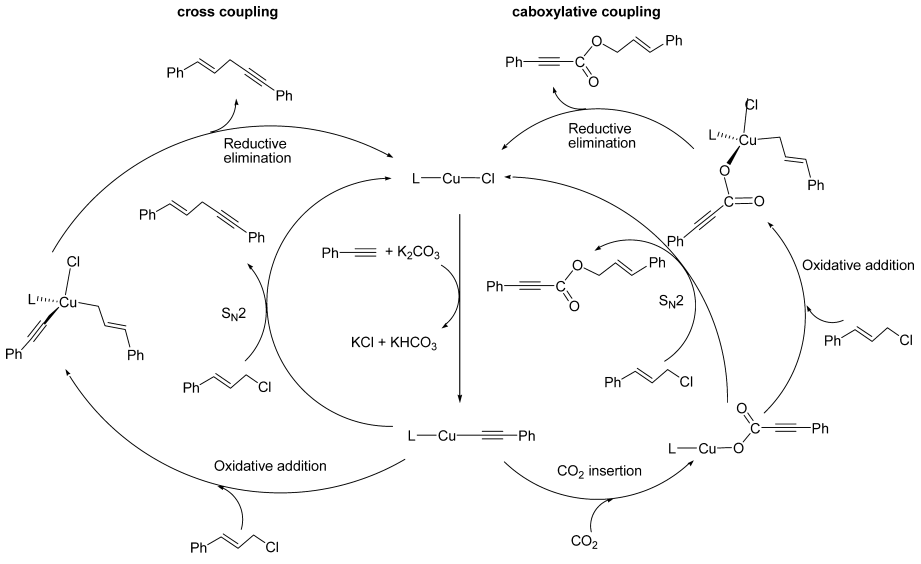

dx.doi.org/10.1021/cs5011184 | ACS Catal. 2014, 4, 4466−4473

overall barrier calculated for cross coupling is 24.8 kcal/mol (B3P86) versus 15.0 kcal/mol (B3P86-D2).

In summarizing all of the above, we conclude that the B3P86-D2 results cannot explain the competitive nature of the reactions. Furthermore, the reaction barriers predicted by the B3P86-D2 method seem a bit too low in view of the experimental temperature (60 °C). B3P86-D2 overestimates the stability of the transition states, especially rate-determining transition state TS_{3-10} for the cross-coupling pathway. We also employed other dispersion-corrected DFT methods, such as BP86-D3, B3PW91-D3, B3LYP-D3 and M06, to re-evaluate the energies of key intermediates (**3** and **6**) and transition states (TS_{3-6}, TS_{6-7}, and TS_{3-10}). The relative energies calculated for these key intermediates and transition states using these dispersion-corrected DFT methods are listed in Table S2. The results again show that the inclusion of the dispersion correction significantly overestimates the stability of transition state TS_{3-10} for the cross-coupling pathway. Therefore, throughout the article we use the B3P86 results for our discussion.

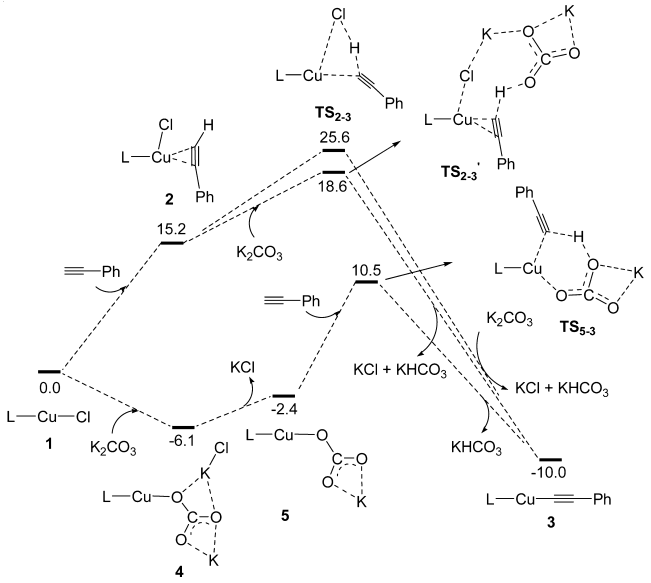

Figure 1. Energy profile calculated for the metathesis reaction between LCuCl (L = IPr) and PhC≡CH leading to the formation of copper(I) acetylide intermediate **3**. The free energies are given in kcal/mol.

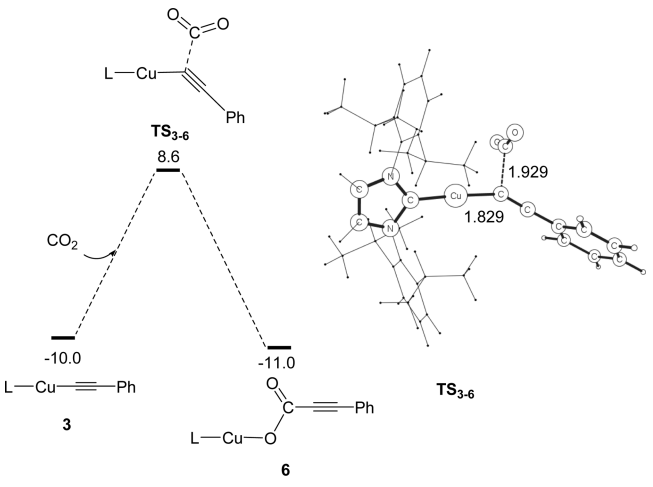

Figure 2. Energy profile calculated for the CO_2 insertion into the copper(I)−acetylide bond in LCuCCPh (**3**) to form carboxylate intermediate **6**. The structure calculated for TS_{3-6} is shown on the right-hand side. The free energies are given in kcal/mol, and the bond lengths are given in angstroms.

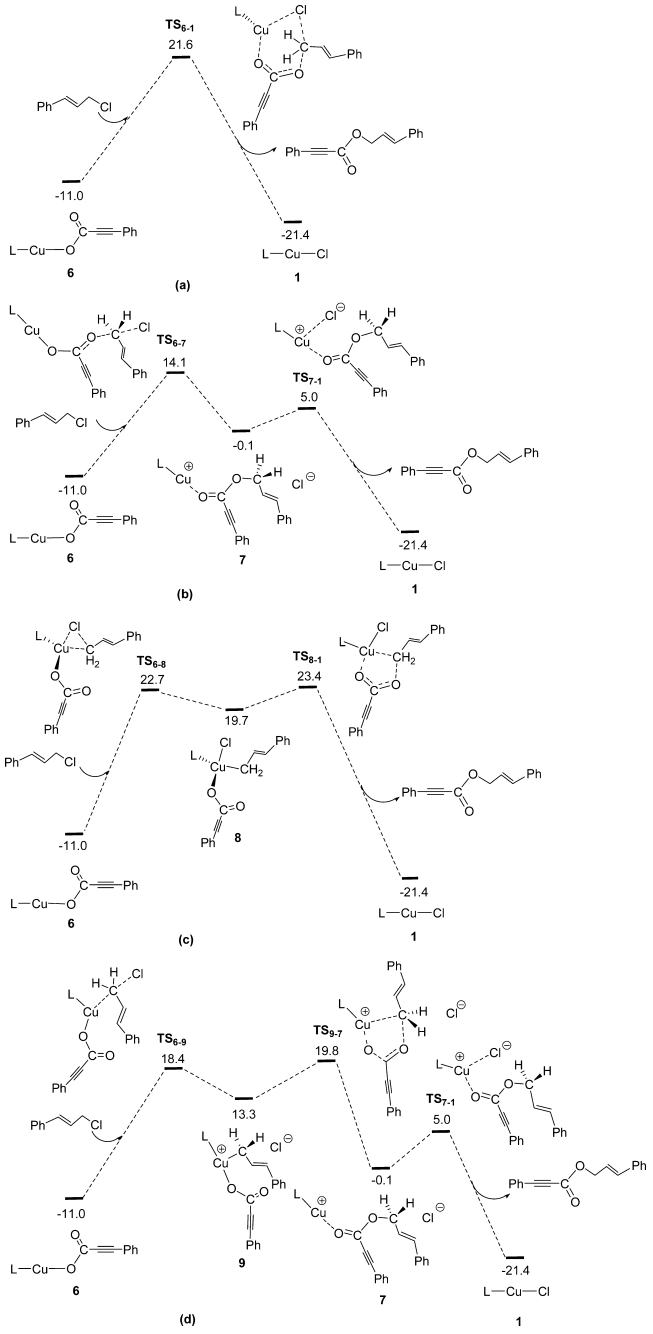

Figure 3. Energy profiles calculated for the reaction of copper(I) carboxylate intermediate **6** with allylic chloride via (a) a concerted S_N2 reaction pathway, (b) a stepwise S_N2 reaction pathway, (c) a traditional oxidative-addition reaction pathway, and (d) a nontraditional oxidative-addition reaction pathway. The free energies are given in kcal/mol.

RESULTS AND DISCUSSION

Metathesis of LCuCl with PhC≡CH to Give LCuC≡CPh: The Role of the Base. Scheme 2 gives a detailed version of the reaction mechanisms shown in Scheme 1. Detailed pathways regarding how copper(I) acetylide intermediate LCuC≡CPh reacts with CO_2 and with the allylic chloride are given in this detailed version.

dx.doi.org/10.1021/cs5011184 | ACS Catal. 2014, 4, 4466−4473

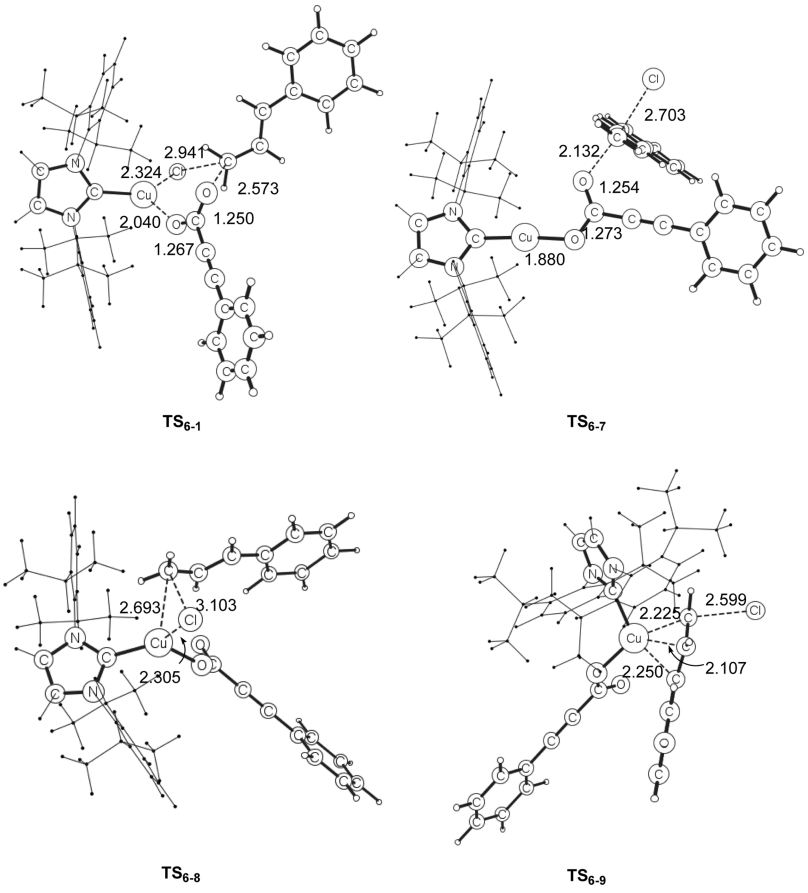

Figure 4. Calculated structures for selected transition states related to the pathways for the reaction of copper(I) carboxylate intermediate **6** with allylic chloride. Bond lengths are given in angstroms.

Before we discuss the detailed mechanism, let us first focus on the first step, which is the metathesis reaction between LCuCl and PhC≡CH to form the copper(I) acetylide intermediate. Figure 1 shows the energy profile calculated for this step. Two pathways were calculated, a direct pathway and a base-assisted pathway.

In the direct pathway, the phenylacetylene substrate molecule coordinates to the LCuCl copper(I) center to form an η^2 complex (**2**) from which proton migration to the chloride ligand occurs followed by an acid−base neutralization (HCl + K_2CO_3 → KCl + $KHCO_3$) to give copper(I) acetylide intermediate **3**. In this direct pathway, the overall free-energy barrier to complete the metathesis via transition state TS_{2-3} was calculated to be 25.6 kcal/mol. The possibility of adding a base (K_2CO_3) to η^2 complex **2** for deportation was also considered (Figure 1). This pathway via transition state TS_{2-3}' (18.6 kcal/mol) is slightly more favorable.

In the base-assisted pathway, a ligand exchange of carbonate (K_2CO_3) for chloride occurs easily to give a thermodynamically more stable double salt of (KCl)(LCuCOOK) that has the structure of **4** shown in Figure 1. Separation of KCl from the double salt gives LCuCOOK (**5**). From **5**, a proton transfer from PhC≡CH to one carbonate oxygen via a six-membered-ring transition state (TS_{5-3}) produces copper(I) acetylide intermediate **3**. As shown in Figure 1, the overall free-energy barrier calculated for this base-assisted pathway is 16.6 kcal/mol, which is much lower than that calculated for the direct pathway. Clearly, the base (K_2CO_3) plays an important role in promoting/facilitating the formation of copper(I) acetylide intermediate **3**.

We also calculated the energetics associated with the direct reactions of LCuCl with CO_2 and allylic chloride. The free-energy barrier for LCuCl + CO_2 → LCuOC(O)Cl was calculated to be 29.3 kcal/mol with a reaction free energy of 28.8 kcal/mol. The reaction free energies for LCuCl + PhCH═CHCH$_2$Cl → [LCu(CH$_2$═CHCHClPh)]Cl and LCuCl + PhCH═CHCH$_2$Cl → LCuCHPhCHClCH$_2$Cl were calculated to be 28.0 and 48.9 kcal/mol, respectively. All of these results indicate that LCuCl will react preferentially with PhC≡CH over CO_2 or allylic chloride.

Carboxylative Coupling. As shown in Schemes 1 and 2, once the copper(I) acetylide intermediate (**3**) is formed, it can react with either CO_2 or allylic chloride to leading to carboxylative coupling or cross coupling. Let us first discuss the carboxylative coupling.

Figure 2 shows the energy profile calculated for the CO_2 insertion into the copper(I)−acetylide bond in **3** to form copper(I) carboxylate intermediate **6**. The overall free energy barrier via TS_{3-6} was calculated to be 18.6 kcal/mol. In the insertion process, the metal-bonded sp-hybridized carbon in intermediate **3** can be viewed as a nucleophile to attack the electrophilic CO_2 carbon center. In transition state TS_{3-6}, the C−C bond being formed is 1.929 Å.

The next step after the CO_2 insertion is that allylic chloride reacts with copper(I) carboxylate intermediate **6**. Reaction of allylic chloride with **6** can proceed either through S_N2 substitution or through oxidative addition followed by reductive elimination.

dx.doi.org/10.1021/cs5011184 | ACS Catal. 2014, 4, 4466−4473

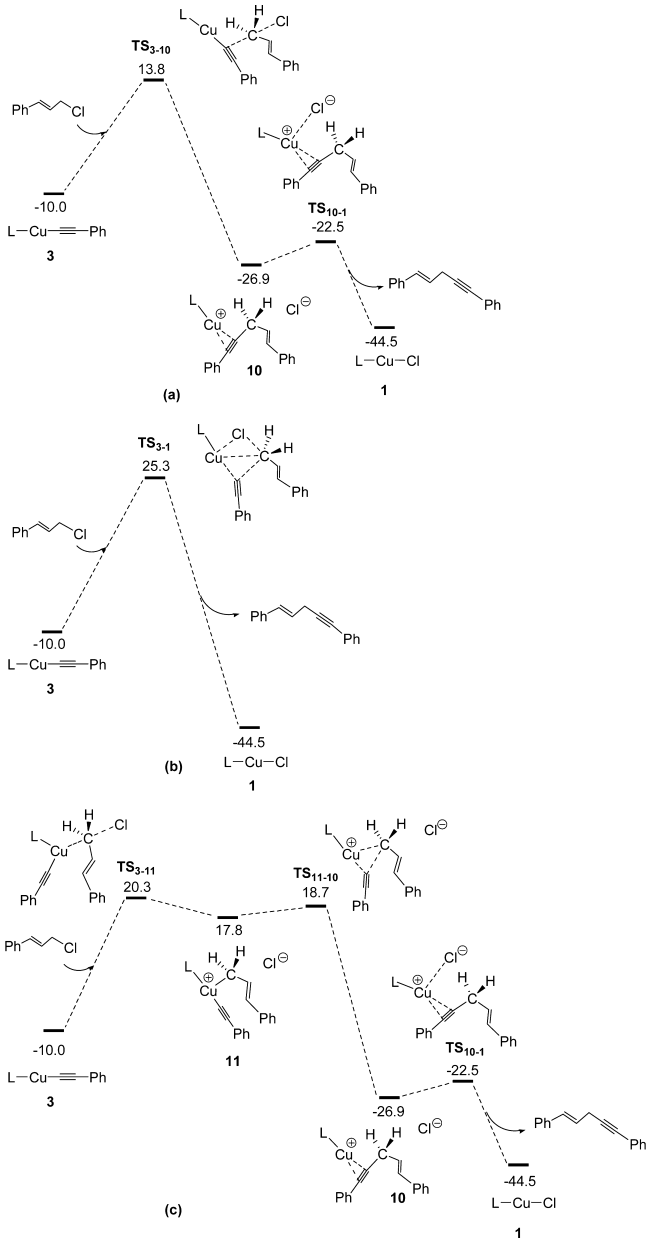

Figure 5. Energy profiles calculated for the reaction of copper(I) acetylide intermediate **3** with allylic chloride via (a) an S_N2 substitution pathway, (b) one-step oxidative addition followed by a reductive-elimination pathway, and (c) a nontraditional oxidative-addition pathway. The free energies are given in kcal/mol.

Figure 3 shows the energy profiles for various possible pathways calculated for the reaction of allylic chloride with copper(I) carboxylate intermediate **6**. Figure 4 gives selected transition-state structures calculated along the reaction pathways studied.

In the S_N2 substitution, there are two possible pathways in which the uncoordinated carboxylate oxygen in **6** acts as the entering group. Figure 3a,b shows the energy profiles calculated for these two possible S_N2 pathways. The pathway shown in Figure 3a is a concerted pathway in which the leaving group (chloride) finds coordination with the copper(I) metal center via six-membered-ring transition state TS_{6-1}. The pathway shown in Figure 3(b) is a stepwise pathway in which the leaving chloride is far away from the metal center and an ion pair (**7**) is formed via the transition state TS_{6-7}.

When oxidative addition is considered, the traditionally seen oxidative addition mode through an η^2 approach of the C−Cl bond toward the copper(I) metal center gives a high reaction barrier of 33.7 kcal/mol (Figure 3c) because of steric hindrance as a result of the bulky IPr ligand. Interestingly, we also found a nontraditional oxidative-addition pathway via transition state TS_{6-9} (Figure 3d) resembling an S_N2 substitution where the metal center acts as an entering group to give an ion pair (**9**) formed between a T-shaped copper(III) complex cation and a chloride anion. From **9**, reductive elimination occurs via another nontraditional reductive elimination transition state (TS_{9-7}) to give ion pair **7**. A structural reorganization in ion pair **7** gives the carboxylative-coupling product and regenerates active species **1**. The overall barrier for this pathway (Figure 3d) was calculated to be 30.8 kcal/mol (**6** → TS_{9-7}).

On the basis of the calculated energy profiles shown in Figure 3, we can conclude that the stepwise S_N2 substitution pathway (Figure 3b) is the most favorable pathway for copper(I) carboxylate intermediate **6** reacting with allylic chloride. The overall free-energy barrier is calculated to be 25.1 kcal/mol (**6** → TS_{6-7}). In considering Figures 1, 2, and 3(b), we can see that C−O bond formation (**6** → TS_{6-7}) is the rate-determining step in the whole carboxylative-coupling reaction. We also note that the overall carboxylative-coupling reaction, PhC≡CH + CO_2 + PhCH═CHCH$_2$Cl + K_2CO_3 → PhC≡CCOOCH$_2$CH═CHPh + $KHCO_3$ + KCl, is exergonic by 21.4 kcal/mol, which is thermodynamically very favorable.

Cross Coupling. In the cross coupling, copper(I) acetylide intermediate **3**, which was formed from the metathesis of LCuCl with PhC≡CH, reacts directly with allylic chloride. Three pathways were calculated for **3** reacting with allylic chloride (Figure 5), i.e., an S_N2 substitution pathway (Figure 5a), one-step oxidative addition followed by reductive-elimination pathway (Figure 5b), and a nontraditional oxidative-addition reaction pathway (Figure 5c). Figure 6 gives selected transition-state structures calculated along the reaction pathways studied.

In the S_N2 substitution pathway (Figure 5a), the acetylide ligand in **3** acts as the entering group to attack the allylic chloride-bonded carbon nucleophilically via transition state TS_{3-10} to form an ion pair (**10**). Then a structural reorganization in the ion pair gives the cross-coupling product and regenerates active species **1**.

In the one-step oxidative addition followed by reductive-elimination pathway (Figure 5b), an oxidatively added four-center transition state (TS_{3-1}) corresponds to oxidative addition of the C−Cl bond to the Cu(I) metal center followed by reductive elimination to give the cross-coupling product and regenerate active species **1** with a barrier of 35.3 kcal/mol. One-step processes involving both oxidative addition and reductive elimination have also been observed in a number of copper-mediated/catalyzed C−C bond-formation reactions.[22]

Similar to what we found for the carboxylative-coupling reaction, a nontraditional oxidative-addition pathway was found via TS_{3-11} to form an ion pair (**11**) between a T-shaped copper(III) complex cation and a chloride anion, from which reductive elimination occurs through TS_{11-10} to give ion pair **10**. Finally, a structural reorganization releases the cross-coupling product and regenerates active species **1**. The overall barrier for this pathway (Figure 5c) was calculated to be 30.3 kcal/mol.

Among the three cross-coupling pathways calculated, the S_N2 substitution pathway (Figure 5a) is clearly the most favorable. In considering Figures 1 and 5a, we can see that C−C bond

dx.doi.org/10.1021/cs5011184 | ACS Catal. 2014, 4, 4466−4473

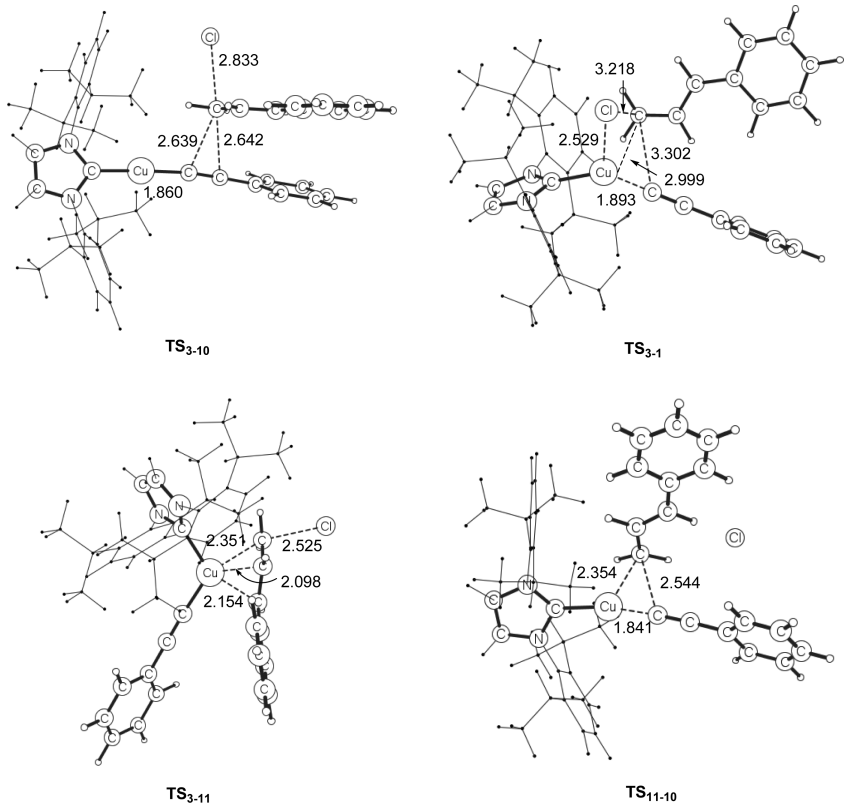

Figure 6. Calculated structures for selected transition states related to the pathways for the reaction of copper(I) acetylide intermediate **3** with allylic chloride. Bond lengths are given in angstroms.

formation via TS_{3-10} is rate-determining for the whole cross-coupling reaction. We also note that the overall cross-coupling reaction, PhC≡CH + PhCH═CHCH$_2$Cl + K_2CO_3 → PhC≡CCH$_2$CH═CHPh + $KHCO_3$ + KCl, is exergonic by 44.5 kcal/mol, which is also thermodynamically very favorable.

Carboxylative Coupling versus Cross Coupling. Figure 7 compares the most favorable pathways calculated for the carboxylative-coupling and cross-coupling reactions discussed above. In the figure, we see that the two highest energy species (TS_{6-7} and TS_{3-10}) have similar stabilities (14.1 versus 13.8 kcal/mol), indicating that the two pathways are highly competitive. These results are consistent with the experimental findings that in general both carboxylative-coupling and cross-coupling products were observed.

Effects of Temperature and Pressure. From Figure 7, we can clearly see that the relative height of TS_{6-7} and TS_{3-10} determines the reaction selectivity of carboxylative coupling versus cross coupling. Carboxylative coupling is a three-component reaction whereas cross coupling is a two-component reaction. The entropy decrease for the former is more significant than that for the latter. Therefore, we expect that the effects of temperature and pressure are more significant for the former than for the latter.

To examine the temperature and pressure effect quantitatively, we evaluated the difference in the relative free energies between the two relevant transition states TS_{6-7} and TS_{3-10} in the respective carboxylative-coupling and cross-coupling reactions at different temperature and pressure (Table 1). The results given in Table 1 indeed show that increasing the pressure and decreasing the temperature increase the energy difference between transition states TS_{6-7} and TS_{3-10} in favor of the carboxylative coupling. Although decreasing the temperature can increase the reaction selectivity for carboxylative coupling, at the same time it decreases the reaction rate. If we assume the Arrhenius equation for the rate constant, then the rate at 273 K is approximately 64 times slower than that at 333 K. Equation 1 shows that the reactions studied were carried out at 333 K for 1 day. We expect that if the reactions were carried out at 273 K then it would take 64 days for the reactions to be completed, which is unrealistic. The experimental condition of 333 K and 1.5 MPa leads to TS_{6-7} being 1.1 kcal/mol lower in free energy than TS_{3-10} (12.4 vs 13.5 kcal/mol), making the carboxylative-coupling product the major product as observed experimentally.

Table 1. Relative Free Energies of the Two Competing Transition States TS_{6-7} and TS_{3-10} in the Respective Carboxylative Coupling and Cross-Coupling Reactions Calculated at Different Temperatures and Pressures[a]

reaction condition		
temperature (K)	pressure (MPa)	$\Delta\Delta G^{\ddagger}\{\Delta G^{\ddagger}(TS_{3-10}) - \Delta G^{\ddagger}(TS_{6-7})\}$ (kcal/mol)
298	0.1	−0.3
	1.5	1.8
	2.0	1.9
333	0.1	−0.7
	1.5	1.1
	2.0	1.3
368	0.1	−1.6
	1.5	0.3
	2.0	0.5

[a]The energy differences between these two relative free energies are given in kcal/mol.

dx.doi.org/10.1021/cs5011184 | ACS Catal. 2014, 4, 4466−4473

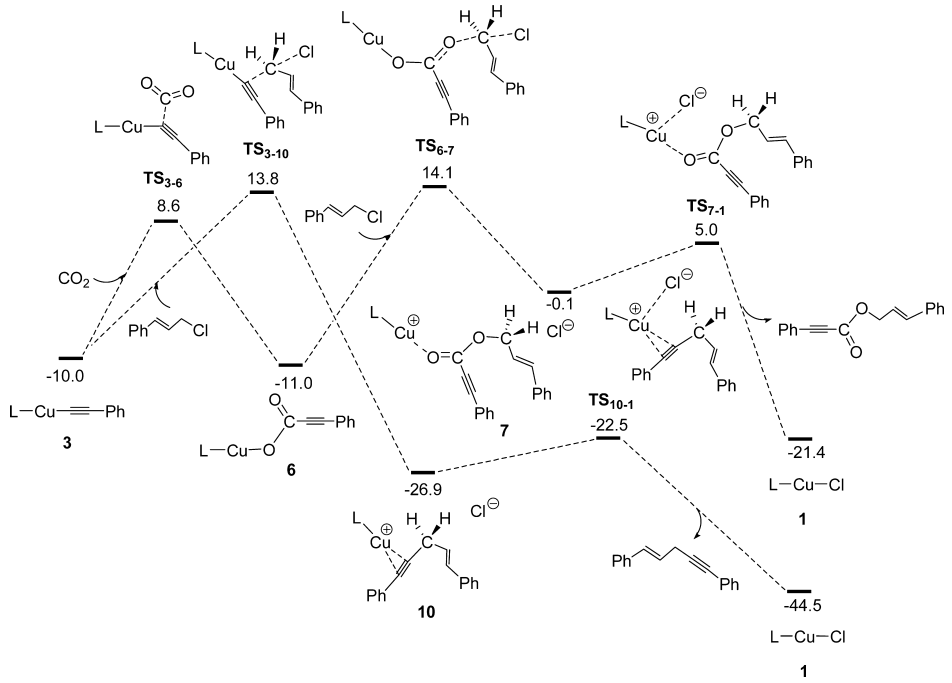

Figure 7. Energy profiles calculated for the most favorable methods of the carboxylative-coupling and cross-coupling reactions. The free energies are given in kcal/mol.

CONCLUSIONS

The detailed mechanisms for carboxylative-coupling reactions among terminal alkynes, allylic chlorides, and CO_2 catalyzed by N-heterocyclic carbene copper(I) complex (IPr)CuCl have been studied with the aid of DFT calculations. At the same time, the competing cross-coupling reactions between terminal alkynes and allylic chlorides have also been investigated. In both the carboxyltive-coupling and cross-coupling reactions, the first step is the metathesis of (IPr)CuCl + PhC≡CH → (IPr)Cu−C≡CPh + HCl, leading to the formation of copper(I) acetylide intermediate (IPr)Cu−C≡CPh. Our calculation results show that in this metathesis step, the base (K_2CO_3) plays an important role in promoting/facilitating formation of the copper(I) acetylide intermediate (IPr)Cu−C≡CPh.

In carboxylative coupling, CO_2 insertion into the copper−acetylide bond of copper(I) acetylide intermediate (IPr)Cu−C≡CPh occurs to give copper(I) carboxylate (IPr)CuOC(O)C≡CPh. Instead of following the expected mechanism of oxidative addition of the allylic chloride C−Cl bond followed by reductive elimination, copper(I) carboxylate reacts with an allylic chloride molecule, via an S_N2 substitution mode through a nucleophilic attack of the uncoordinated carboxylate oxygen on the chloride-bonded carbon of the allylic chloride molecule, to give the carboxylative-coupling product (carboxylic ester) and regenerate active species (IPr)CuCl.

In the cross coupling, copper(I) acetylide intermediate (IPr)Cu−C≡CPh directly reacts with the allylic chloride. The calculations again indicate that the reaction mechanism does not follow the expected oxidative addition followed by reductive elimination. Similar to what we found in the carboxylative coupling, the reaction occurs again via an S_N2 substitution mode through a nucleophilic attack of the acetylide copper-bonded carbon onto the chloride-bonded carbon of the allylic chloride molecule to give the cross-coupling product and regenerate active species (IPr)CuCl.

Our calculation results show that the S_N2 transition states are the rate-determining transition states for both the carboxylative-coupling and cross-coupling reactions. In addition, the two S_N2 transition states show similar stabilities; therefore, the two reactions are actually competitive.

The carboxylative coupling is a three-component reaction whereas the cross-coupling reaction is a two-component reaction. Considering the entropy effect, we deduce that high pressure and low temperature will benefit the carboxylative reactions. The calculation results and the experimental observations support this conclusion.

ASSOCIATED CONTENT

Supporting Information

The following file is available free of charge on the ACS Publications website at DOI: 10.1021/cs5011184.

Relative free energies calculated for key intermediates and transition states using various dispersion-corrected DFT methods and Cartesian coordinates and electronic energies for all of the calculated structures (PDF)

AUTHOR INFORMATION

Corresponding Author

*E-mail: chzlin@ust.hk.

Notes

The authors declare no competing financial interest.

ACKNOWLEDGMENTS

This work was supported by the Research Grants Council of Hong Kong (GRF 16303614) and the National Natural Science Foundation of China (21203156).

REFERENCES

(1) (a) Hileman, B. *Chem. Eng. News.* **1995**, *27*, 18−23. (b) Hileman, B. *Chem. Eng. News.* **1997**, *17*, 9−10.

(2) (a) Cooney, C. M. *Environ. Sci. Technol.* **1997**, *31*, 576A−576A. (b) Zurer, P. S. *Chem. Eng. News.* **1995**, *13*, 27−30. (c) Magrini, K. A.; Boron, D. *Chem. Ind.* **1994**, 997−1000. (d) Farla, J. C. M.; Hendriks, C. A.; Blok, K. *Climat. Change.* **1995**, *29*, 439−461. (e) Yin, X. *J. Environ. Sci.* **1995**, *7*, 129−137. (f) Edwards, J. H. *Catal. Today.* **1995**, *23*, 59−66. (g) Markewitz, P.; Kuckshinrichs, W.; Leitner, W.; Linssen, J.; Zapp, P.; Bongartz, R.; Schreiber, A.; Müller, T. E. *Energy Environ. Sci.* **2012**, *5*, 7281−7305. (h) Wang, W.; Wang, S.; Ma, X.; Gong, J. *Chem. Soc. Rev.* **2011**, *40*, 3703−3727. (i) Yu, K. M. K.; Curcic, I.; Gabriel, J.; Tsang, S. C. E. *ChemSusChem* **2008**, *1*, 893−899. (j) Mikkelsen, M.; Jørgensen, M.; Krebs, F. C. *Energy Environ. Sci.* **2010**, *3*, 43−81. (k) Omae, I. *Coord. Chem. Rev.* **2012**, *256*, 1384−1405.

(3) (a) Sakakura, T.; Choi, J. C.; Yasuda, H. *Chem. Rev.* **2007**, *107*, 2365−2387. (b) Sakakura, T.; Kohon, K. *Chem. Commun.* **2009**, 1312−1330. (c) Cokoja, M.; Bruckmeier, C.; Rieger, B.; Herrmann, W. A.; Kühn, F. E. *Angew. Chem., Int. Ed.* **2011**, *50*, 8510−8537. (d) Decortes, A.; Castilla, A. M.; Kleij, A. W. *Angew. Chem., Int. Ed.* **2010**, *49*, 9822−9837.

(4) (a) Louie, J. *Curr. Org. Chem.* **2005**, *9*, 605−623. (b) Aresta, M.; Dibenedotto, A. *Dalton Trans.* **2007**, *28*, 2975−2992. (c) Baiker, A. *Appl. Organometal. Chem.* **2000**, *14*, 751−762.

(5) (a) Yin, X.; Moss, J. R. *Coord. Chem. Rev.* **1999**, *181*, 27−59. (b) Riduan, S. N.; Zhang, Y. *Dalton Trans.* **2010**, *39*, 3347−3357. (c) Darensbourg, D. J. *Inorg. Chem.* **2010**, *49*, 10765−10780. (d) Zhang, L.; Cheng, J.; Ohishi, T.; Hou, Z. *Angew. Chem., Int. Ed.* **2010**, *49*, 8670−8673. (e) Yang, Z. Z.; Zhao, Y. N.; He, L. N. *RSC Adv.* **2011**, *1*, 545−567. (f) Ohishi, T.; Zhang, L.; Nishiura, M.; Hou, Z. *Angew. Chem., Int. Ed.* **2011**, *50*, 8114−8117. (g) Mansell, S. M.; Kaltsoyannis, N.; Arnold, P. L. *J. Am. Chem. Soc.* **2011**, *133*, 9036−9051. (h) Kumar, S.; Kumar, P.; Jain, S. L. *RSC Adv.* **2013**, *3*, 24013−24016. (i) Bontemps, S.; Sabo-Etienne, S. *Angew. Chem., Int. Ed.* **2013**, *52*, 10253−10255. (j) Zhang, Y.; Hanna, B. S.; Dineeen, A.; Williard, P. G.; Bernskoetter, W. H. *Organometallics* **2013**, *32*, 3969−3979. (k) Horn, B.; Limberg, C.; Herwig, C.; Braun, B. *Chem. Commun.* **2013**, *49*, 10923−10925.

(6) (a) Ukai, K.; Aoki, M.; Takaya, J.; Iwasawa, N. *J. Am. Chem. Soc.* **2006**, *128*, 8706−8715. (b) Takaya, J.; Tadami, S.; Ukai, K.; Iwasawa, N. *Org. Lett.* **2008**, *10*, 2697−2700. (c) Ohishi, T.; Nishiura, M.; Hou, Z. *Angew. Chem., Int. Ed.* **2008**, *47*, 5792−5795.

(7) (a) Boogaerts, I. I. F.; Nolan, S. P. *Chem. Commun.* **2011**, *47*, 3021−3024. (b) Boogaerts, I. I. F.; Nolan, S. P. *J. Am. Chem. Soc.* **2010**, *132*, 8858−8859. (c) Huang, K.; Sun, C. L.; Shi, Z. J. *Chem. Soc. Rev.* **2011**, *40*, 2435−2452. (d) Yeung, C. S.; Dong, V. M. *J. Am. Chem. Soc.* **2008**, *130*, 7826−7827. (e) Kobayashi, K.; Kondo, Y. *Org. Lett.* **2009**, *11*, 2035−2037. (f) Williams, C. M.; Johnson, J. B.; Rovis, T. *J. Am. Chem. Soc.* **2008**, *130*, 14936−14937. (g) Correa, A.; Martín, R. *J. Am. Chem. Soc.* **2009**, *131*, 15974−15975. (h) Mizuno, H.; Takaya, J.; Iwasawa, N. *J. Am. Chem. Soc.* **2011**, *133*, 1251−1253. (i) Yu, D. Y.; Zhang, Y. G. *Green Chem.* **2011**, *13*, 1275−1279. (j) Saito, S.; Nakagawa, S.; Koizumi, T.; Hirayama, K.; Yamamoto, Y. *J. Org. Chem.* **1999**, *64*, 3975−3978. (k) Shimizu, K.; Takimoto, M.; Sato, Y.; Mori, M. *Org. Lett.* **2005**, *7*, 195−197. (l) Aoki, M.; Kaneko, M.; Izumi, S.; Ukai, K.; Iwasawa, N. *Chem. Commun.* **2004**, 2568−2569.

(8) (a) Zhang, S. Lin.; Liu, L.; Fu, Y.; Guo, Q. X. *Organometallics* **2007**, *26*, 4546−4554. (b) Dang, L.; Lin, Z.; Marder, T. B. *Organometallics* **2010**, *29*, 917−927. (c) Xue, L.; Lin, Z. *Chem. Soc. Rev.* **2010**, *39*, 1692−1705. (d) Uhe, A.; Hölscher, M.; Leitner, W. *Chem.—Eur. J.* **2012**, *18*, 170−177. (e) Lau, K. C.; Petro, B. J.; Bontemps, S.; Jordan, R. F. *Organometallics* **2013**, *32*, 6895−6898.

(9) (a) Fukue, Y.; Oi, S.; Inoue, Y. *J. Chem. Soc. Chem. Commun.* **1994**, *18*, 2091−2091. (b) Inamoto, K.; Asano, N.; Kobayashi, K.; Yonemoto, M.; Kondo, Y. *Org. Biomol. Chem.* **2012**, *10*, 1514−1516. (c) Yu, B.; Diao, Z. F.; Guo, C. X.; Zhong, C. L.; He, L. N.; Zhao, Y. N.; Song, Q. W.; Liu, A. H.; Wang, J. Q. *Green Chem.* **2013**, *15*, 2401−2407. (d) Inomata, H.; Ogata, K.; Fukuzawa, S.; Hou, Z. M. *Org. Lett.* **2012**, *14*, 3986−3989. (e) Manjolinho, F.; Arndt, M.; Gooßen, K.; Gooßen, L. J. *ACS Catal.* **2012**, *2*, 2014−2021.

(10) Zhang, W. Z.; Li, W. J.; Zhang, X.; Zhou, H.; Lu, X. B. *Org. Lett.* **2010**, *12*, 4748−4751.

(11) Vechorkin, O.; Hirt, N.; Hu, X. *Org. Lett.* **2010**, *12*, 3567−3569.

(12) (a) Thasana, N.; Worayuthakarn, R.; Kradanrat, P.; Hohn, E.; Young, L.; Ruchirawat, S. *J. Org. Chem.* **2007**, *72*, 9379−9382. (b) Sun, C.; Fang, Y.; Li, S.; Zhang, Y.; Zhao, Q.; Zhu, S.; Li, C. *Org. Lett.* **2009**, *11*, 4084−4087. (c) Davies, K. A.; Abel, R. C.; Wulff, J. E. *J. Org. Chem.* **2009**, *74*, 3997−4000. (d) Bieber, L. W.; da Silva, M. F. *Tetrahedron Lett.* **2007**, *48*, 7088−7090.

(13) (a) Yao, X. Q.; Hou, X. J.; Wu, G. S.; Xu, Y. Y.; Xiang, H. W.; Jiao, H. J.; Li, Y. W. *J. Phys. Chem. A* **2002**, *106*, 7184−7189. (b) Yao, X. Q.; Hou, X. J.; Jiao, H. J.; Xiang, H. W.; Li, Y. W. *J. Phys. Chem. A* **2003**, *107*, 9991−9996.

(14) (a) Becke, A. D. *Phys. Rev. A* **1988**, *38*, 3098−3100. (b) Perdew, J. P. *Phys. Rev. B* **1986**, *33*, 8822−8824.

(15) (a) McGrath, M. P.; Radom, L. *J. Chem. Phys.* **1991**, *94*, 511−516. (b) Raghavachari, K.; Binkley, J. S.; Seeger, R.; Pople, J. A. *J. Chem. Phys.* **1980**, *72*, 650−654.

(16) (a) Petersson, G. A.; Bennett, A.; Tensfeldt, T. G.; Al-Laham, M. A.; Shirley, W. A.; Mantzaris, J. *J. Chem. Phys.* **1988**, *89*, 2193−2218. (b) Petersson, G. A.; Al-Laham, M. A. *J. Chem. Phys.* **1991**, *94*, 6081−6090.

(17) Tomasi, J.; Mennucci, B.; Cammi, R. *Chem. Rev.* **2005**, *105*, 2999−3093.

(18) de Marothy, S. A. *XYZViewer*, version 0.97; Stockholm, 2010.

(19) (a) Fukui, K. *J. Phys. Chem.* **1970**, *74*, 4161−4163. (b) Fukui, K. *Acc. Chem. Res.* **1981**, *14*, 363−368.

(20) (a) Benson, S. W. *The Foundations of Chemical Kinetics*; Krieger: Malabar, FL, 1982. (b) Okuno, Y. *Chem.—Eur. J.* **1997**, *3*, 212−218. (c) Ardura, D.; López, R.; Sordo, T. L. *J. Phys. Chem. B* **2005**, *109*, 23618−23623. (d) Schoenebeck, F.; Houk, K. N. *J. Am. Chem. Soc.* **2010**, *132*, 2496−2497. (e) Liu, Q.; Lan, Y.; Liu, J.; Li, G.; Wu, Y. D.; Lei, A. *J. Am. Chem. Soc.* **2009**, *131*, 10201−10210. (f) Ariafard, A.; Brookes, N. J.; Stanger, R.; Yates, B. F. *Organometallics* **2011**, *30*, 1340−1349. (g) Yu, H.; Lu, Q.; Dang, Z.; Fu, Y. *Chemistry − An Asian Journal* **2013**, *8*, 8−18. (h) Ariafard, A.; Ghohe, N. M.; Abbasi, K. K.; Canty, A. J.; Yates, B. F. *Inorg. Chem.* **2013**, *52*, 707−717. (i) Fan, T.; Sheong, F. K.; Lin, Z. *Organometallics* **2013**, *32*, 5224−5230. (j) Xie, H.; Lin, Z. *Organometallics* **2014**, *33*, 892−897.

(21) Frisch, M. J.; Trucks, G. W.; Schlegel, H. B.; Scuseria, G. E.; Robb, M. A.; Cheeseman, J. R.; Scalmani, G.; Barone, V.; Mennucci, B.; Petersson, G. A.; Nakatsuji, H.; Caricato, M.; Li, X.; Hratchian, H. P.; Izmaylov, A. F.; Bloino, J.; Zheng, G.; Sonnenberg, J. L.; Hada, M.; Ehara, M.; Toyota, K.; Fukuda, R.; Hasegawa, J.; Ishida, M.; Nakajima, T.; Honda, Y.; Kitao, O.; Nakai, H.; Vreven, T.; Montgomery, Jr., J. A.; Peralta, J. E.; Ogliaro, F.; Bearpark, M.; Heyd, J. J.; Brothers, E.; Kudin, K. N.; Staroverov, V. N.; Kobayashi, R.; Normand, J.; Raghavachari, K.; Rendell, A.; Burant, J. C.; Iyengar, S. S.; Tomasi, J.; Cossi, M.; Rega, N.; Millam, J. M.; Klene, M.; Knox, J. E.; Cross, J. B.; Bakken, V.; Adamo, C.; Jaramillo, J.; Gomperts, R.; Stratmann, R. E.; Yazyev, O.; Austin, A. J.; Cammi, R.; Pomelli, C.; Ochterski, J. W.; Martin, R. L.; Morokuma, K.; Zakrzewski, V. G.; Voth, G. A.; Salvador, P.; Dannenberg, J. J.; Dapprich, S.; Daniels, A. D.; Farkas, Ö.; Foresman, J. B.; Ortiz, J. V.; Cioslowski, J.; Fox, D. J. *Gaussian 09*, Revision D.01; Gaussian, Inc.: Wallingford, CT, 2009.

(22) (a) Wang, M.; Lin, Z. *Organometallics* **2010**, *29*, 3077−3084. (b) Wang, M.; Fan, T.; Lin, Z. *Organometallics* **2012**, *31*, 560−569.